RESEARCH

Projections of meteorological drought events in the upper Kızılırmak basin under climate change scenarios

Sefa Furkan Selçuk[1] · Burcu Çirci Selçuk[2] · Meltem Sarıoğlu Cebeci[3]

Abstract

Climate change, whose negative impacts are becoming increasingly apparent as a result of human actions, intensifies the drought problems to dangerous levels. The development of local-scale drought projections is crucial to take necessary precautions for potential risks and possible effects of drought. In this study, drought analysis was conducted in the Upper Kızılırmak Basin using the standard precipitation index (SPI) method for the near future (2020–2049), mid-century (2050–2074), and late century (2075–2099). The precipitation data required for the SPI were gathered from the data sets developed for the SSP climate change scenarios of the four chosen global climate models. Precipitation data has been made more convenient for local analysis studies with the statistical downscaling method. Forecasts have been created for the temporal variation and spatial distribution of drought events. The study findings indicate that, under the SSP 2-4.5 scenario, drought-related effects of climate change will decrease until 2100. On the other hand, the number and severity of drought events, as well as the duration of dry periods, will increase until 2100 under the SSP 5-8.5 scenario. According to the SSP 5-8.5 scenario, consisting of the most pessimistic forecasts, moderate drought will last 0–60 months, severe drought will last 0–30 months, and extreme drought will last 0–20 months in different regions of the area in the late century. The spatial distribution of droughts will differ based on the SPI index and climate change scenarios. Comparison of SPI and CZI data showed that both indices are effective in meteorological drought analyses.

1 Introduction

Drought is an extreme climate event that involves meteorological and hydrological processes with destructive impacts on water resources, health, economy, energy and food security. The rapid escalation of the effects of human-induced climate change, the rapid decrease of available water resources, and the forecasts of water scarcity have increased the interest in drought studies. The tendency for an increase in global temperatures is expected to bring about significant changes in the intensity and frequency of extreme weather occurrences such as meteorological droughts. While this change is predicted to decrease in some regions of the world, it is anticipated that droughts will become severe in more areas (IPCC 2013). In the Mediterranean climate zone, which also includes the study area, there is a consensus that there is an increasing tendency for drought events (Tramblay et al. 2020; Gudmundsson and Seneviratne 2016; Knutson and Zeng 2018; Kelley et al. 2015). Most climate models predict that the Mediterranean climate zone will face an increase in the intensity of droughts and a northward shift in the region's temperature regimes due to being one of the regions most affected by human-induced climate change (Gomez-Gomez et al. 2022; Bolch et al. 2012).

✉ Sefa Furkan Selçuk
  sefafurkan.selcuk@gmail.com

[1] Faculty of Engineering, Environmental Engineering Department, Artvin Coruh University, Artvin, Turkey

[2] Faculty of Architecture, Fine Arts and Design, Department of City and Regional Planning, Sivas Cumhuriyet University, Sivas, Turkey

[3] Faculty of Engineering, Environmental Engineering Department, Sivas Cumhuriyet University, Sivas, Turkey

The fact that the Kızılırmak basin is one of the largest in Turkey, as well as the fact that the Kızılırmak was formed in Turkey and flowed into the sea in Turkey, gives the basin great importance. According to various studies conducted at the local scale, the regions of Central Anatolia and Eastern Anatolia in Turkey, including the Kızılırmak basin, began to experience drought in 2012. In the following years, the drought intensified and began to affect wider regions (Türkeş 2019). Türkeş (2012), applied the Mann-Kendall trend test to precipitation data for the period of 1950–2010 to examine Turkey's precipitation trends and found that there is a statistically significant decreasing trend in precipitation during the winter months in the region where the Upper Kızılırmak Basin is located. Additionally, the study created a drought index map of Turkey and calculated the drought index for the region containing the Upper Kızılırmak Basin to be below 0.65. Accordingly, the area has been defined as a semi-arid region with an annual water deficit. It is believed that as the effects of global warming increase, droughts will become more severe. In their study, Sen et al. (2012) projected that under the A2 climate change scenario, the drought in the province of Sivas, which includes the upper Kızılırmak basin, will have an insignificant tendency to increase between 2071 and 2100. Selçuk et al. (2022) stated that there was an annual average spatial precipitation distribution of 638–2066 mm in the reference period (1950–2000) in Sivas province and predicted that precipitation would decrease by 0–8%, 4 – 12%, 0–20%, and 4–26%, respectively until 2100 under the climate change scenarios of RCP 2.6, RCP 4.5, RCP 6.0 and RCP 8.5. Afshar et al. (2020), conducted a drought analysis in Ankara, which is geographically close to the upper Kızılırmak basin and has a similar climate, and estimated the changes in drought events that may occur under the RCP 4.5 and RCP 8.5 climate change scenarios. According to the study, there will be an increasing rise in future drought events. Droughts will occur for longer durations, and their frequency and severity will increase. On the other hand, Danandeh Mehr et al. (2020) predicted future drought events in Ankara based on the RCP4.5 and RCP8.5 scenarios for the years between 2016 and 2040. According to the study, extreme drought episodes are not expected in the region under either scenario. However, it is expected that drought events will occur toward the end of the study period based on the RCP 4.5 scenario, while they are projected to occur throughout the study period based on the RCP 8.5 scenario. In light of these studies, it is essential to make drought forecasts in the Upper Kızılırmak basin based on climate change projections for addressing issues such as adaptation to climate change, food security, and sustainable use of water resources.

Global climate models (GCMs) are the most reliable tools used to predict future conditions in studies examining the effects of climate change. In order to use these tools on a local scale, downscaling methods must be used. There are two basic downscaling techniques: dynamic downscaling and statistical downscaling. The biggest disadvantage of the dynamic downscaling technique that limits its use in climate change studies is its complex design and high computational cost (Corell 2007). In addition, it is not flexible in terms of expanding or making changes to the work area, which may require renewal of the entire work (Crane and Hevidson 1998). Statistical downscaling methods, on the other hand, have high computational efficiency.

There are many studies that have conducted drought analysis for the future using climate change scenarios (Danandeh Mehr et al. 2020; Lee et al. 2017; Azizi and Nejatian 2022). However, trend analysis of drought events that are likely to occur under climate change scenarios and mapping of these drought events There is a deficiency in the subject. Trend analysis will provide a better analysis of the effects of climate change by showing the trend of future drought events more clearly. In this study, meteorological drought events that are likely to occur in the future were calculated using the standardized precipitation index (SPI) and drought trends were determined with the modified Mann-Kendall analysis. It is a method that is frequently used in meteorological drought analysis studies and has proven its reliability (Lee et al. 2017; Bong and Richard 2020). Additionally, World Meteorological Organization has recommended SPI as the main meteorological drought index that should be used in monitoring and researching drought events (Hayes et al. 2011). Time series affected by the influence of seasonal variables like SPI exhibit autocorrelation. Since the classic Mann-Kendall method does not effectively address autocorrelation, it can indicate false trends in these time series. Many alternative methods to the Mann-Kendall method have been developed in the literature and tested on different data sets (Kisi and Ay 2014; Hamed and Rao 1998; Hu et al. 2020). In recent studies, the Modified Mann-Kendall (MMK) test has been highlighted as an appropriate method to analyze trends in hydro-meteorological data (Lornezhad et al. 2023).The MMK test's ability to account for serial correlation and changing variance in data series makes it suitable for accurately detecting subtle trends in meteorological data sets (Hamed and Rao 1998).

The present study analysed the drought events expected to occur in the Upper Kızılırmak basin under climate change scenarios. The severity and duration of drought events were calculated using the SPI method, according to the SPI-3 and SPI-12 indexes. The future climate data used in the SPI calculation were gathered from the data sets developed for the SSP (Shared Socio-Economic Pathways) scenarios of four different global climate models. Statistical downscaling was applied to the obtained data. The temporal variation

analysis of drought events was performed by interpreting the graphs of SPI time series and using statistical trend analysis methods. Chinese z index (CZI) values were calculated and compared with SPI values and Pearson correlation test was performed. On the other hand, the spatial distribution analysis of the drought was made through the spatial distribution maps created by the interpolation method using the total number of dry months calculated for different periods. The fact that the study area is already under the impact of drought, the lack of comparable drought-related forecasting studies in the region and the scarcity of similar studies conducted under SSP scenarios in the literature contribute to the importance of this study.

2 Material and method

2.1 Study area

The second largest basin in Turkey, Kızılırmak, is the basin of the country's longest river, which has a length of 1.355 km and originates and flows into the sea within Turkish territory (Ercan and Yüce 2017). The length of the portion of the river (Upper Kızılırmak Basin) within Sivas province is roughly 300 km (Sağdıç and Koç 2012). The general topography of the region causes an increase in height from west to east (Circi Selcuk and Irmak 2022). Figure 1 shows the elevation map of the study area and the grids of the CFSR dataset.

The Upper Kızılırmak region is influenced by the continental climate characterized by cold, wet winters and hot, dry summers. The climate in the region varies depending on the altitude. While the climate is gentler in the lowlands, the average annual temperature drops as proceeding to the mountainside. The average winter temperature is below zero (Sağdıç and Koç 2012). Summer months are typically dry in the region. Most precipitation occurs in spring. While the area receives a lot of snowfall, the annual precipitation occurs mostly in the winter months, following the spring months (Ercan and Yüce 2017).

According to the data of Coordination of Information on the Environment (CORINE) provided by the European Environment Agency (EEA), the largest portion (20%) of the region's land use/cover consists of sparse vegetation. The region is mostly utilized for agriculture and consists of 18% non-irrigated arable land and 14% land with
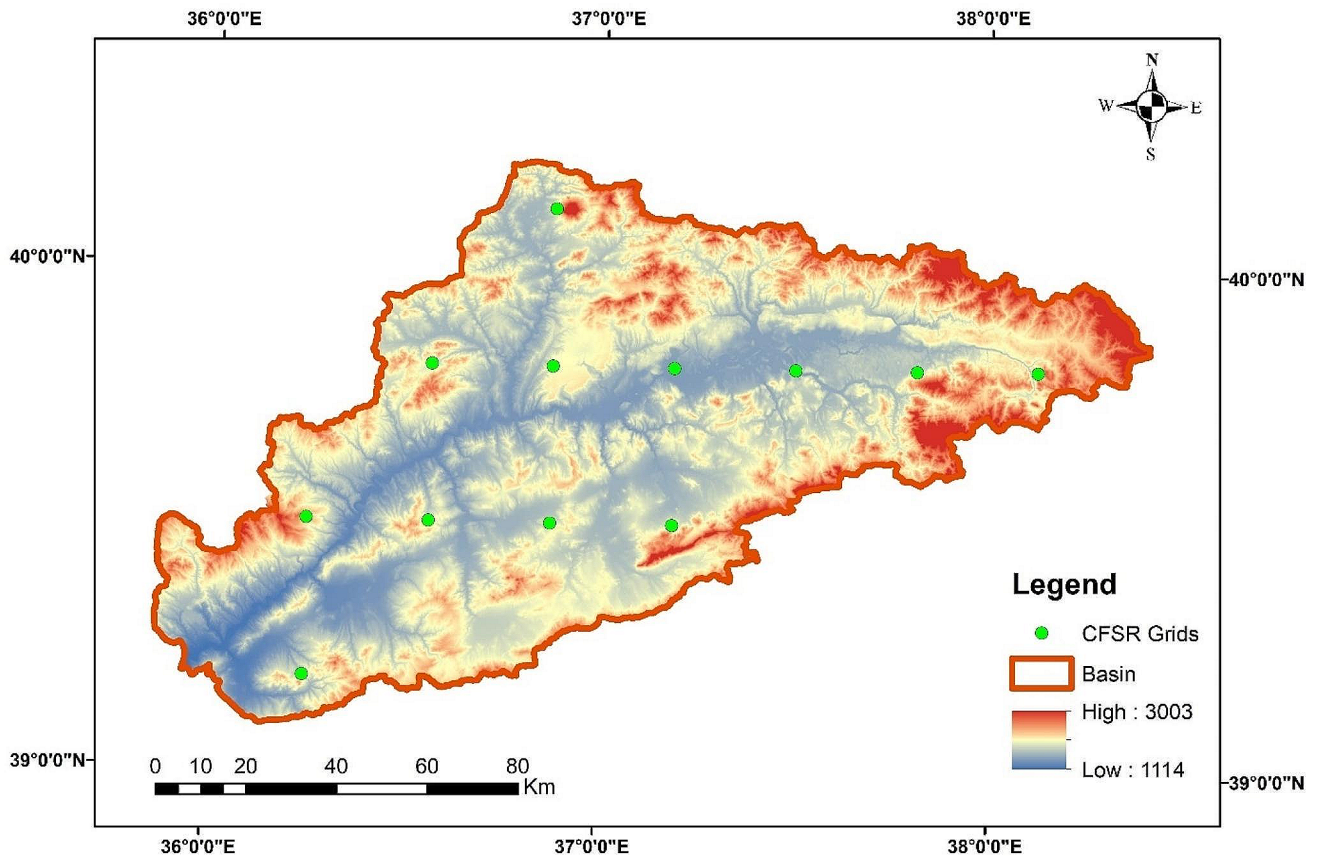

Fig. 1 Upper Kızılırmak basin

natural vegetation. The water bodies cover an area of 0.3% (4252 ha).

2.2 Statistical downscaling method

GCMs are the most reliable tools for obtaining climate data and predicting future conditions in climate change studies. GCMs perform reasonably well for simulating climate variables on a global and continental scale. However, they fall short in regional or local analysis studies. The present study employed the statistical downscaling technique due to its computational efficiency and low cost. Climate Change Toolkit (CCT) (Vaghefi et al. 2017) software was used to apply statistical downscaling and error correction to the data of SSP2-4.5 and SSP5-8.5 climate change scenarios of BCC-CSM2-MR, GFDL-ESM4, INM-CM5-0, and MRI-ESM2 global climate models with 0.9 resolution shared by CMIP6 (Coupled Model Intercomparison Project 6) (Xin et al. 2019; John et al. 2018; Volodin et al. 2019; Yukimoto et al. 2019).

SSPs were published for the first time in 2017 in order to take socioeconomic developments and climate policies into account while developing climate scenarios. They were developed by merging the greenhouse gas reduction scenarios of the RCP scenarios with the socio-economic development scenarios such as population, economic growth, education, urbanization, and the pace of technological development. There are 5 different SSPs defined. These are SSP1 (sustainability), SSP2 (middle of the road), SSP3 (regional rivalry), SSP4 (inequality), and SSP5 (rapid growth). In our study, SSP2-4.5 and SSP5-8.5 scenarios have been preferred because they are more likely to occur, have the same levels of radiative forcing as the previous scenarios, RCP 4.5 and RCP 8.5, and are more comparable to the literature. The SSP2-4.5 scenario represents socio-economic developments with moderate challenges for mitigation of climate change and adaptation. This scenario predicts that the radiative forcing will reach 4.5 W/m^2 by 2100. On the other hand, the SSP5-8.5 scenario depicts socioeconomic developments in which rapid fossil fuel development will take place, with high difficulties in mitigation and low-level difficulties in adaptation. In this scenario, the radiative forcing level is predicted to reach 8.5 W/m^2 by 2100 (IPCC 2021).

The downscaling module of the CCT software requires local measurement data for downscaling. The module uses the statistical bias correction method, the most commonly employed statistical downscaling method (Vaghefi et al. 2017). In this method, the data is transferred to this station by applying bias correction to the grid data of the global climate model that is nearest to the station whose measurement data is defined. This method has been considered satisfactory in various climatological studies (Asong et al. 2016; Dosio and Paruolo 2011; Hagemann et al. 2011).

The software applies a correction factor based on Eq. 1 to the temperature data for monthly periods (Vaghefi et al. 2017).

$$T_{corrected_{ij}} = T_{GCM_{ij}} + (\bar{T}_{reference_{jk}} - \bar{T}_{GCM_{jk}}) \qquad (1)$$

In Eq. 1, T represents temperature, $\bar{T}$ long-term mean temperature, and i, j,k represent the day, month, and year, respectively. For precipitation data, the software uses the multiplicative correction factor in Eq. 2 (Vaghefi et al. 2017).

$$P_{corrected_{ij}} = P_{GCM_{ij}} * \frac{\bar{P}_{Reference_{jk}}}{\bar{P}_{GCM_{jk}}} \qquad (2)$$

In Eq. 2, P represents precipitation, $\bar{P}$ long-term mean precipitation, and i, j, and k represent the day, month, and year, respectively.

There are three local measurement stations within the borders of the basin where long-time (> 20 years) measurements are taken. Due to the insufficiency of local measurement data in the study area, it was decided to utilize the CFSR (Climate Forecast System Reanalysis) data set with a scale of 0.25°, which is frequently and effectively used in statistical downscaling studies (Timbal et al. 2009; Blanco-Gómez et al. 2019; Singh and Kumar 2020; Ndhlovu and Woyessa 2021; Anuchaivong et al. 2017; Selçuk et al. 2022).

The CFSR dataset is a third-generation reanalysis product developed by NCEP (The National Centers for Environmental Prediction). It was designed and executed as a global, high-resolution, and coupled atmosphere-ocean-land surface-sea ice system. The global land surface model has 4 soil levels and the global sea ice model has 3 levels. The CFSR atmospheric model contains observed variations in carbon dioxide (CO_2), together with changes in aerosols and other trace gases and solar energy. Precipitation data were obtained from the data set for the 1979–2014 time periods with a grid resolution of 0.25° and on a daily time scale (Saha et al. 2010; Dile and Srinivasan 2014). Four global climate model datasets with a scale of 0.9° are downscaled to a scale of 0.25°. Figure 1 illustrates the grid structure resulting from downscaling. In order to be less impacted by the uncertainties of global climate models, studies were continued by averaging the data from multiple global climate models.

2.3 Drought analysis

The standardized precipitation index (SPI) method, one of the most utilized methods for analyzing droughts, was employed in the study. A measurement point must have precipitation data spanning at least 30 years for SPI calculation. This long-term precipitation data, which is the only source of input used in the calculation, is first adapted to a gamma probability distribution (Eq. 3), and then it is converted to a standard normal variable (Eq. 4) (Edwards and McKee 1997).

$$g(x) = \frac{1}{\beta^{\alpha} \Gamma(\alpha)} x^{\alpha-1} e^{-x/\beta} \tag{3}$$

In Eq. 3, α represents shape parameter, β represents scale parameter, $\Gamma(\alpha)$ represents gamma function and x represents precipitation amount.

$$SPI_{ij} = \frac{x_{ij} - x?_j}{\sigma_j} \tag{4}$$

In Eq. 4, x_{ij} represents precipitation, $\bar{x}_j$ represents the mean precipitation and σ_j represents the standard deviation in month j of the year i.

This method is used to determine the periods and degrees of drought or abnormal precipitation events with changes in precipitation over a long-term scale. The SPI depicts the deviations of the total precipitation value from the mean for the analyzed accumulation period. Positive SPI values indicate more precipitation than the average amount of precipitation, while negative SPI values indicate less precipitation than the average amount of precipitation. SPI values less than or equal to -1 indicate drought (McKee et al. 1993). The drought classifications determined based on SPI values are listed in Table 1. The magnitude of the deviation from the mean is a probabilistic measure of the anomaly significance.

In order to determine the prospective effects of the anomalies, calculations can be performed for accumulation periods of 1, 3, 6, 12, 24, and 48 months. Calculations for short accumulation periods provide an indicator of the effects of the anomaly on soil moisture, whereas calculations for long accumulation periods provide an indicator of the effects on groundwater and water reserves. In the study, calculations were made for the SPI-3 and SPI-12 accumulation periods.

Table 1 Drought classifications (McKee et al. 1993)

SPI values	Drought category
-1.0 ≥ SPI > -1.5	Moderate drought
-1.5 ≥ SPI > -2.0	Severe drought
-2.0 ≥ SPI	Extreme drought

The SPI-Generator software developed by the National Drought Mitigation Center (University of Nebraska-Lincoln) was used to determine SPI-3 and SPI-12 values of 12 grids that were generated through downscaling. In the study area, the general condition of the potential drought was determined by averaging the data calculated for twelve separate points. Evaluations are based on the time series generated by the SPI-3 and SPI-12 drought events for the near future (2020–2049), mid-century (2050–2074), and late century (2075–2099) for the SSP2-4.5 and SSP5-8.5 scenarios. Sen's Slope and modified Mann-Kendall analyses were used to conduct trend analyses on the generated time series.

Moreover, spatial analysis of potential future drought was conducted by calculating the total number of months experiencing drought in moderate drought, severe drought, and extreme drought classifications based on the SPI-3 and SPI-12 indexes. The number of drought-affected months is computed separately for the near future, mid-century, and late century under the SSP2-4.5 and SSP5-8.5 climate change scenarios. The spatial distribution maps of the data were created by applying geographic information system software and the inverse distance weighting (IDW) method to these data.

In the study, CZI values were also calculated to verify the SPI values and make a comparison. Correlation test was performed for SPI and CZI values. The China Z-Index (CZI) is a method extensively used by the National Climate Center (NCC) of China to assess the country's drought conditions (Wu et al. 2001). In this index, it is assumed that precipitation data follow the Pearson Type III distribution, and it is based on the assumption that chi-square distributed variables are transformed to the Z-score scale through the Wilson–Hilferty cube root transformation (Kendall and Stuart 1977), and it is calculated according to Eqs. 5–7.

$$\sigma = \sqrt{\frac{1}{n} \sum_{i=1}^{ii} (x_i - \bar{x})^2} \tag{5}$$

$$C_{st} = \frac{\sum_i^n (x_i - \bar{x})^3}{n * \sigma^3} \tag{6}$$

$$CZI = \frac{6}{C_{st}} \sqrt[3]{\frac{C_{st}}{2} ZScore_t + 1} - \frac{6}{C_{st}} + \frac{C_{st}}{6} \tag{7}$$

Here, C_{st} is the coefficient of skewness for any time scale t (1, 3, 6, 9, 12 and 24 months), σ is the standard deviation, n is the observation period.

2.4 Trend analysis

Modified Mann-Kendall and Sen's Trend Tendency tests are non-parametric statistical analysis methods that are commonly employed to determine upward or downward trends in hydrological, meteorological, and climatological time series (Merabti et al. 2018; Zhang et al. 2012; Lornezhad et al. 2023). These methods were employed in the study to analyze trends in drought events that were predicted to take place in the future. Modified Mann-Kendall test statistic is calculated according to Eq. 8 (Mann 1945; Kendall 1975; Hamed and Rao 1998).

$$S = \sum_{i=1}^{n-1} \sum_{j=i+1}^{n} sgn(x_j - x_i) \tag{8}$$

In the equation, n represents the number of data, and x_j and x_i represent x_i, ..., x_n data. Positive S values represent upward trends, whereas negative S values represent downward trends. The variance of the S value is calculated based on Eq. 9, and the standardized modified Mann-Kendall statistics is calculated based on Eq. 12.

$$Var(S) = 1/18[n(n-1)(2n+5)$$
$$- \sum_{i=1}^{m} t_i(t_i-1)(2t_i+5)] \tag{9}$$

$$Var(S)^* = Var(S)\frac{n}{n^*} \tag{10}$$

$$\frac{n}{n^*} = 1 + \frac{2}{n(n-1)(n-2)}$$
$$\sum (n-k)(n-k-1)(n-k-2)r_k^R \tag{11}$$

where $\frac{n}{n^*}$ represents the correction factor, r_k^R represents the lag-k serial correlation coefficient of the ranks, m represents the number of relative groups in the data set and t_i stands for the connected observations in a series of length i.

$$Z = \begin{cases} \frac{S-1}{\sqrt{var(S)^*}}, & S > 0 \\ 0, & S = 0 \\ \frac{S+1}{\sqrt{var(S)^*}}, & S < 0 \end{cases} \tag{12}$$

The trend in drought events was estimated using Sen's trend method. According to the method, the estimation of the mean trend is made using Eq. 13 and Eq. 14 (Sen 1968).

$$Q_i = \frac{x_j - x_k}{j - k} \text{for} i = 1, ..., N \tag{13}$$

$$N = n(n-1)/2 \tag{14}$$

Here n represents the number of time periods and the data at times of j and, k provided that x_j and x_k are $j > k$. The N values of Q_i are sorted from smallest to largest, and if N is an even number, Q_{med} is calculated with Eq. 15, and if N is an odd number, it is calculated with Eq. 16.

$$Q_{med} = Q_{(N+1)/2} \tag{15}$$

$$Q_{med} = \frac{1}{2}\left(Q_{N/2} + Q_{(N+2)/2}\right) \tag{16}$$

3 Findings and discussion

3.1 Temporal change analysis of drought

The present study applied statistical downscaling to four different global climate data sets in order to analyze possible future drought events in the Upper Kızılırmak basin. In order to minimize the uncertainties in the small-scale data sets obtained, they were averaged and converted into a single data set. On the basis of these data sets, the SPI-3 and SPI-12 indexes were calculated for the SSP2-4.5 and SSP5-8.5 climate change scenarios, and drought analyses were conducted for the near future, mid-century and late century.

For the general drought analysis, data that can represent the entire study area were created by averaging of the data from the points in the area where data were collected. Modified Mann-Kendall and Sen trend estimation methods were employed for drought event trend analysis, and the results are presented in Tables 2 and 3. SPI time series were analyzed with the help of the graphs created in Figs. 2, 3, 4 and 5.

The presence of trends in drought events was evaluated with the modified Mann-Kendall test at a significance level of 0.05. In light of this, it is accepted that when the condition $z \geq 1.96$ is met, there is a statistically significant decrease trend in drought events, and when $z \leq -1.96$ is met, there is a statistically significant increase trend in drought events. When the SSP2-4.5 climate change scenario is considered, it is determined that would not be a statistically significant trend in SPI values in the analyzed periods (Table 2). According to the SPI-3 index, if the SSP5-8.5 scenario is realized, there will be an decreasing trend of drought events with a Sen's slope (Q_{med}) value of 0.00205 in the mid-century. According to the SPI-12 index, there will be a decreasing trend in drought events with a Sen's slope (Q_{med}) value of 0.00090 in mid-century (Table 3).

Fig. 2 SPI-3 index time series according to SSP2-4.5 scenario
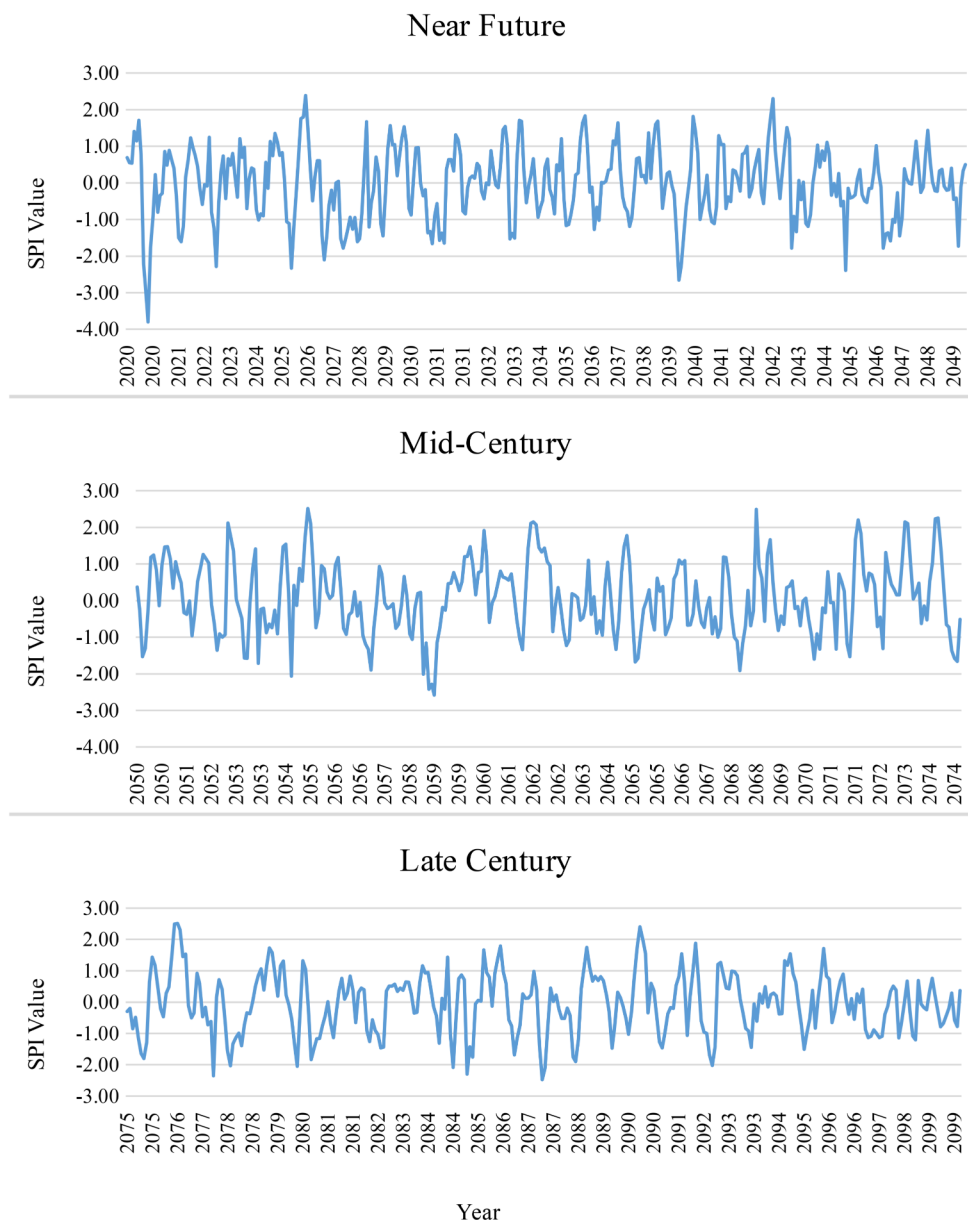

Figure 2 illustrates SPI-3 time series created according to the SSP2-4.5 scenario. Examining Fig. 2 reveals that extreme drought events will occur rarely, their incidence will decrease from the near future to the end of the century, and the duration of extreme drought will be short. It is observed that the fluctuations in the created time series for the near future are quite frequent. In this period, rainfall and drought periods will be short. By the mid-century, the number of months with droughts will decline and the periods with above-average rains will lengthen. In the graph for the late century, it can be observed that the SPI-3 values reached zero near the end of the investigation period. In this period, precipitation anomalies will decrease to almost non-existent.

When the drought analysis is conducted using the SPI-12 index belonging to the SSP2-4.5 scenario, it is observed that the SPI-12 index responds to changes in precipitation more slowly compared to the SPI-3 (Fig. 3). The number of cases where SPI-12 is negative or positive is very few compared to SPI-3. However, periods of drought and rain are considerably longer. In the near future, the most probable drought event is expected to last from month 78 to month 105 during the analyzed period. During this dry period, the SPI-12 value is predicted to peak at -2.79 and then decline. Similar to the SPI-3 time series graph, it is seen that the anomalies occurred in the SPI-12 will decrease considerably as the end of the century approaches.

Figure 4 displays the graph of the SPI-3 index time series created by the most pessimistic climate change scenario,

Fig. 3 SPI-12 index time series according to SSP2-4.5 scenario

Near Future

Mid-Century

Late Century

Year
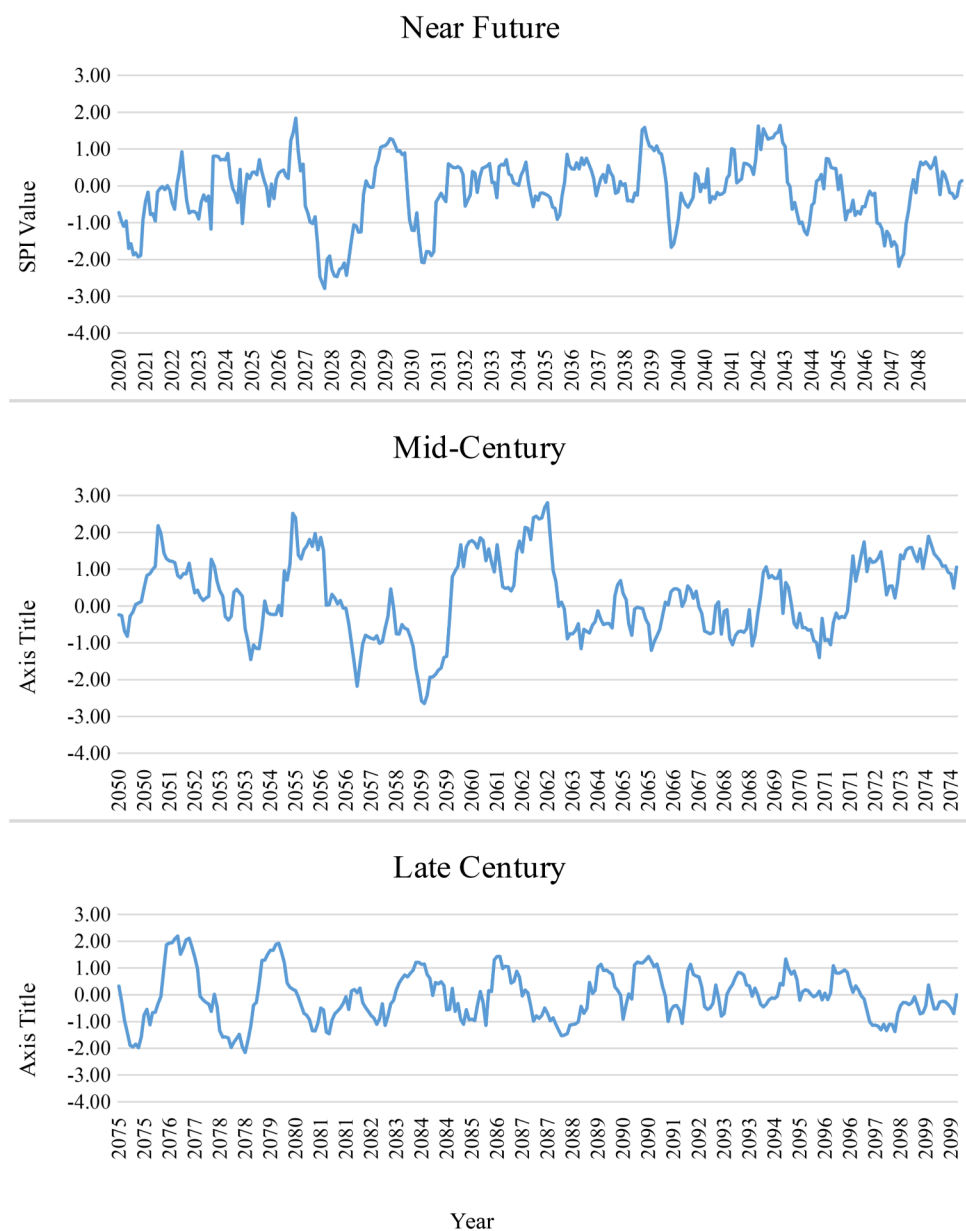
SSP5-8.5. The graph indicates that, in the near future, there will be significantly fewer drought anomalies in the SSP5-8.5 scenario compared to the SSP2-4.5. This is due to the fact that SPI values are calculated as deviations from the mean precipitation. No significant drought anomalies are expected, especially until the middle of the near future. On the other hand, the frequency and severity of drought events, which began in the middle of the near future, will increase in the mid-century due to the consequences of climate change, and there will be more extreme drought problems compared to the SSP2-4.5 scenario. Moreover, it is predicted that drought anomalies will occur with an SPI-3 value of -4, the dry periods getting longer, and the frequency and severity of which increase considerably in the late century. According

to research made for the province of Ankara, which is geographically close to the Upper Kızılırmak basin and shares similar climatic characteristics, it is reported that the number, severity, and duration of drought events will increase (Afshar et al. 2020; Danandeh Mehr et al. 2020). These findings are also consistent with the predictions made for the Mediterranean climate zone (IPCC 2013).

Figure 5 depicts the SPI-12 time series graphs created for the SSP5-8.5 scenario. Similar to the SPI-3 time series, calculations based on SSP5-8.5 indicate that there will be fewer drought anomalies in the SPI-12 in the near future compared to SSP2-4.5. Furthermore, it has been predicted that the number and severity of drought anomalies that are likely to be experienced in the mid-century and the length

Fig. 4 SPI-3 index time series
according to SSP5-8.5 scenario
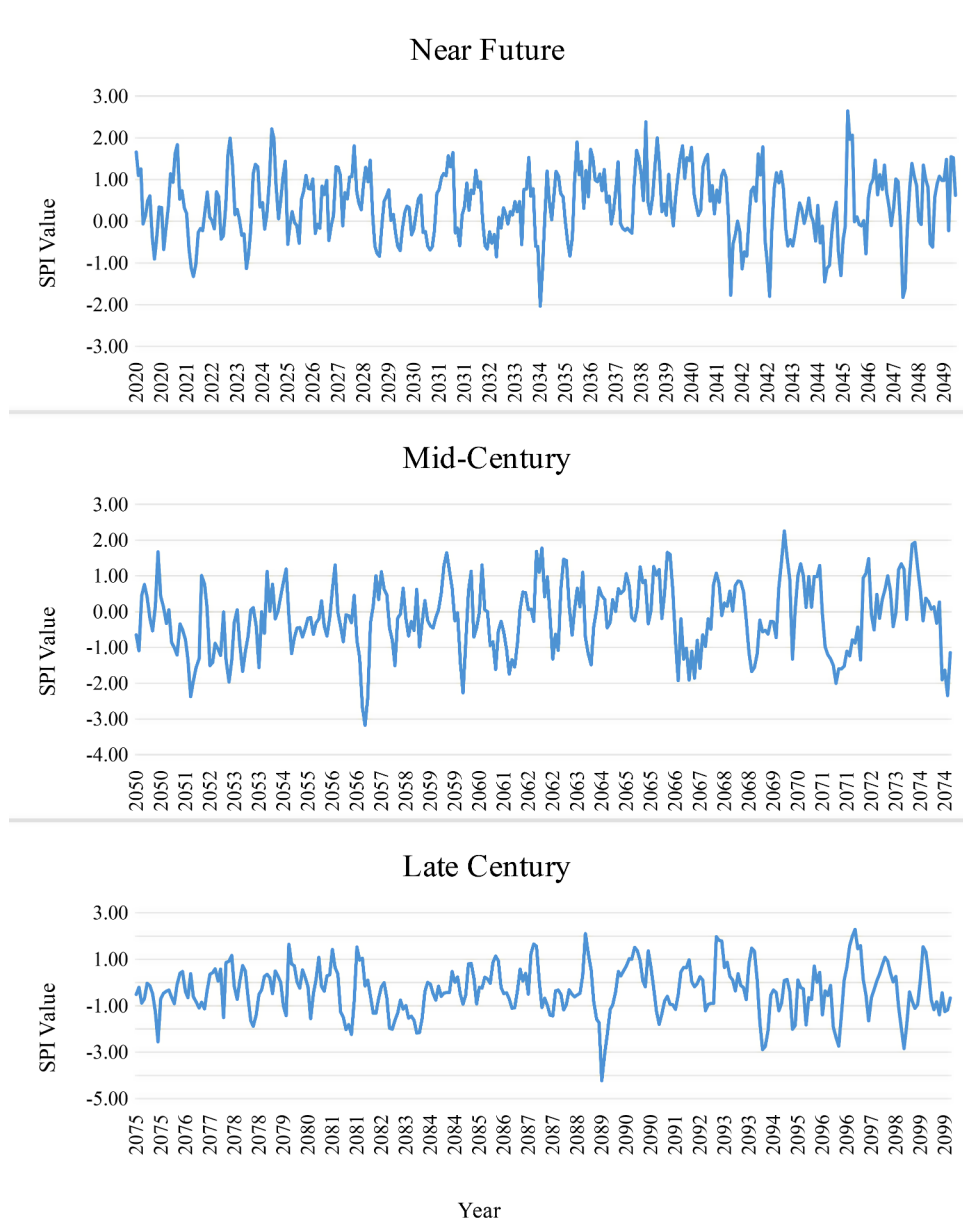
of drought periods will increase. Examining the graph that was created for the late century reveals that there will not be a significant drought anomaly for a long period of time (until the 94th month), which is rather remarkable. After this non-dry period, a drought anomaly is predicted to last for approximately 22 months and peak at SPI-12 value −2.60. This anomaly represents the most important drought event predicted by the SPI-12 index. Sen et al. (2012), according to the SPI-12 index, anticipated that between 2071 and 2100, Sivas will experience a non-significant increase in drought under the A2 climate change scenario. SSP5-8.5 can be compared to climate change scenario A2 as their values are similar. It is predicted that the trend analysis created for the relevant period and conditions in our study will not reveal a statistically significant increase. However, based

on Fig. 5, the fact that SPI-12 values are mostly negative beginning in the 73rd month suggests that there will be an increase, although this is not statistically significant.

SPI-3 is used to capture short-term drought events and is generally associated with agricultural drought. The analysis conducted in the Upper Kızılırmak Basin shows that short-term drought trends according to the SPI-3 index are sensitive to seasonal variations. Especially, an increase in drought events during the summer months has been detected, which can be attributed to a decrease in precipitation during this period. SPI-3 effectively captures these short-term changes, providing important information for agricultural planning and water resources management.

On the other hand, SPI-12 evaluates longer-term drought trends and is generally associated with hydrological drought.

Fig. 5 SPI-12 index time series according to SSP5-8.5 scenario

Near Future

Mid-Century
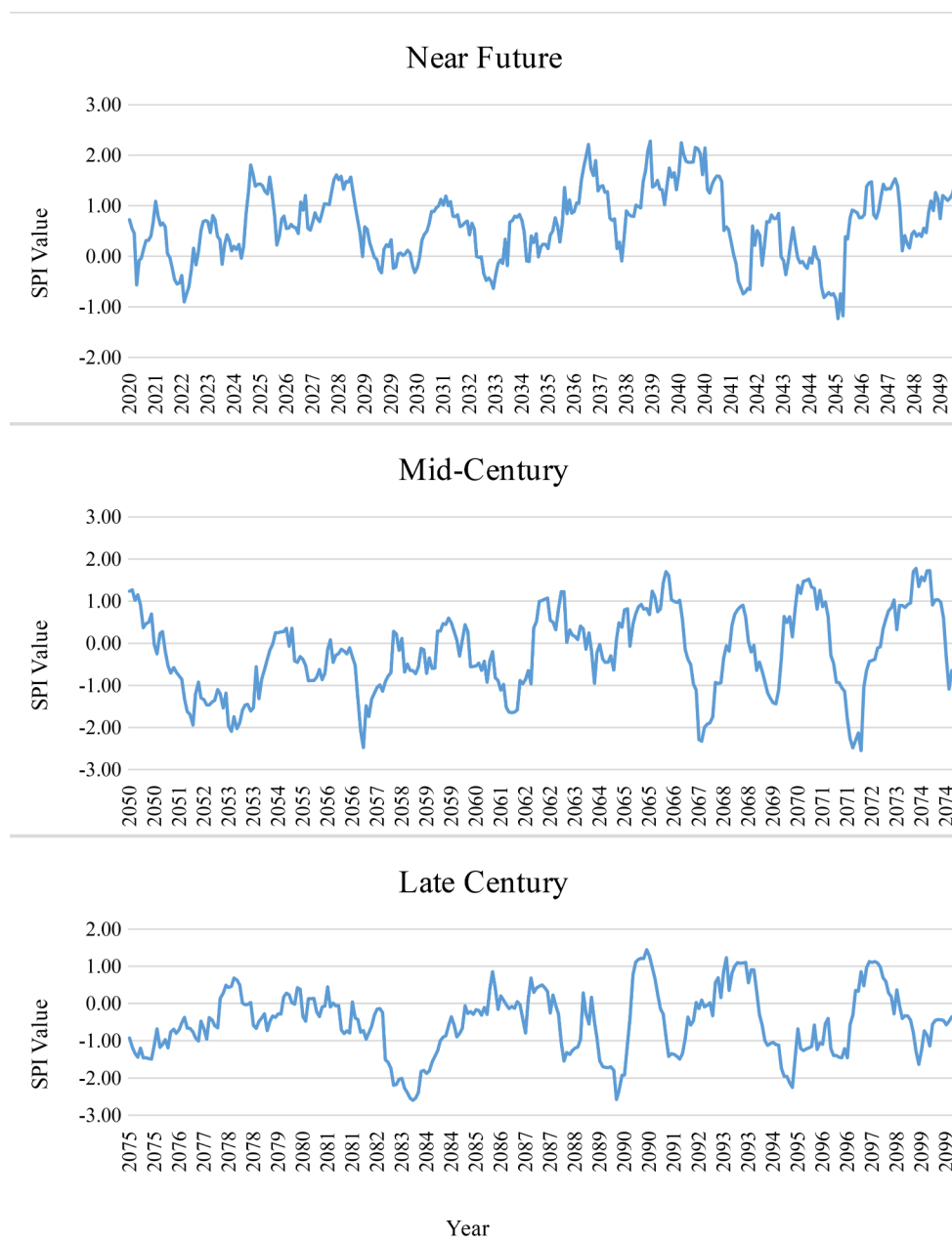
Late Century

Table 2 Trend analysis results for the SSP2-4.5 scenario

	SPI-3			SPI-12		
	Near Future	Mid-Century	Late Century	Near Future	Mid-Century	Late Century
Alpha	0.05	0.05	0.05	0.05	0.05	0.05
n/n*	0.4744	1.4761	2.8201	4.6808	5.2417	3.2051
Z-stat	-0.3465	-0.3399	-0.2322	0.9226	0.4216	0.3307
Trend	no	no	no	no	no	no
Sen's slope	-0.000125	-0.000287	-0.000265	0.000936	0.000718	0.000393

Table 3 Trend analysis results for the SSP5-8.5 scenario

	SPI-3			SPI-12		
	Near Future	Mid-Century	Late Century	Near Future	Mid-Century	Late Century
Alpha	0.05	0.05	0.05	0.05	0.05	0.05
n/n*	1.5742	0.4988	0.6617	2.9958	0.3153	2.4735
Z-stat	0.7965	4.2674	0.2570	1.5768	10.8803	1.0353
Trend	no	yes	no	no	yes	no
Sen's slope	0.000429	0.00205	0.000137	-0.00270	0.00090	-0.00048

Table 4 Pearson correlation coefficients

SSP2-4.5 scenario		SSP5-8.5 scenario	
SPI-3 and CZI-3	SPI-12 and CZI-12	SPI-3 and CZI-3	SPI-12 and CZI-12
0.997081	0.999289	0.99543	0.999107

Our SPI-12 analysis reveals that long-term drought events in the Upper Kızılırmak Basin occur on a broader scale and generally span multiple hydrological years. This indicates the pressures on the long-term water cycle in the basin and potential stresses on water resources. SPI-12 is of critical importance in water management and planning, especially for dams and water storage facilities.

3.2 Comparison of SPI and CZI values

SPI and CZI, calculated based on precipitation data, are two significant indicators widely used in drought research. While SPI measures the normalized deviation of long-term precipitation data for a specific time period at a location, CZI determines the intensity of drought considering the skewness of the precipitation distribution. Both indices offer effective tools for defining and categorizing meteorological drought conditions.

In the study, SPI and CZI values were calculated from precipitation data obtained from the same measuring station to validate the accuracy of SPI data comparatively with CZI. This validation process aims to enhance the reliability of the drought analysis used in the study. A Pearson correlation test has been performed to statistically establish the similarity between the calculated SPI and CZI values. The computed Pearson correlation coefficients are presented in Table 4. Coefficient values being very close to +1 indicate an almost perfect positive linear relationship between SPI and CZI values. Furthermore, Figs. 6 and 7 provide the time series of SPI and CZI values. The figures demonstrate that SPI and CZI data exhibit similar trends and can produce consistent results. This similarity proves that both indices are reliable tools for determining drought conditions and classifying drought severity. Moreover, the comparison between SPI and CZI is a significant step in enhancing the accuracy and comprehensiveness of drought risk assessments necessary for drought management and water resources planning.

3.3 Spatial distribution of drought

Spatial distribution analysis of possible future drought events in the study area was conducted over the spatial distribution maps of the number of experienced dry months. Separate maps were created for moderate, severe and extreme drought events.

Figure 8 shows the spatial distribution maps of the number of experienced moderately dry months based on SPI-3 and SPI-12 on different periods and climate change scenarios. Under the SSP2-4.5 scenario, according to the SPI-3 index, a drought of 30–35 months will be experienced in most of the study area in the near future, while a drought of 35–40 months will be experienced in the region where Kızılırmak originates in the east of the basin. In the mid-century, it is expected that the region will experience a drought that will last for 25–30 months. In the late century, it is expected that the region will experience a moderate drought that will last for 30–35 months in the western part of the study area and 20–25 months in the eastern part. In the near future, the SPI-12 index indicates that droughts will last for 15–20 months in the northwest, 30–35 months in the east, and 20–25 months in the remaining center region. Drought events, expected to be experienced for 10–15 months in the center region in the mid-century, are expected to increase towards the eastern and western ends. It is predicted that there will be a moderate drought of 30–35 months at the western end of the area and 20–25 months at the eastern end. In the late century, it is anticipated that there will be a moderate drought lasting 30–35 months in the southwestern region and 35–40 months in the region comprising around 70% of the remaining study area.

According to the SPI-3 index, the SSP5-8.5 scenario predicts a moderate drought lasting 0–10 months in the western region, 10–15 months in the central region, and 15–20 months in the eastern region in the near future. The study area is expected to experience a drought lasting 30–35 months in the mid-century, and the region will have a drought lasting 30–35 months in the late century, with some areas of the central region experiencing a drought lasting 35–40 months. According to the SPI-12 index, a drought lasting 0–10 months is expected in the entire study area in the near future. It is predicted that, in the mid-century, there will be

Fig. 6 SPI and CZI index time series according to SSP2-8.5 scenario
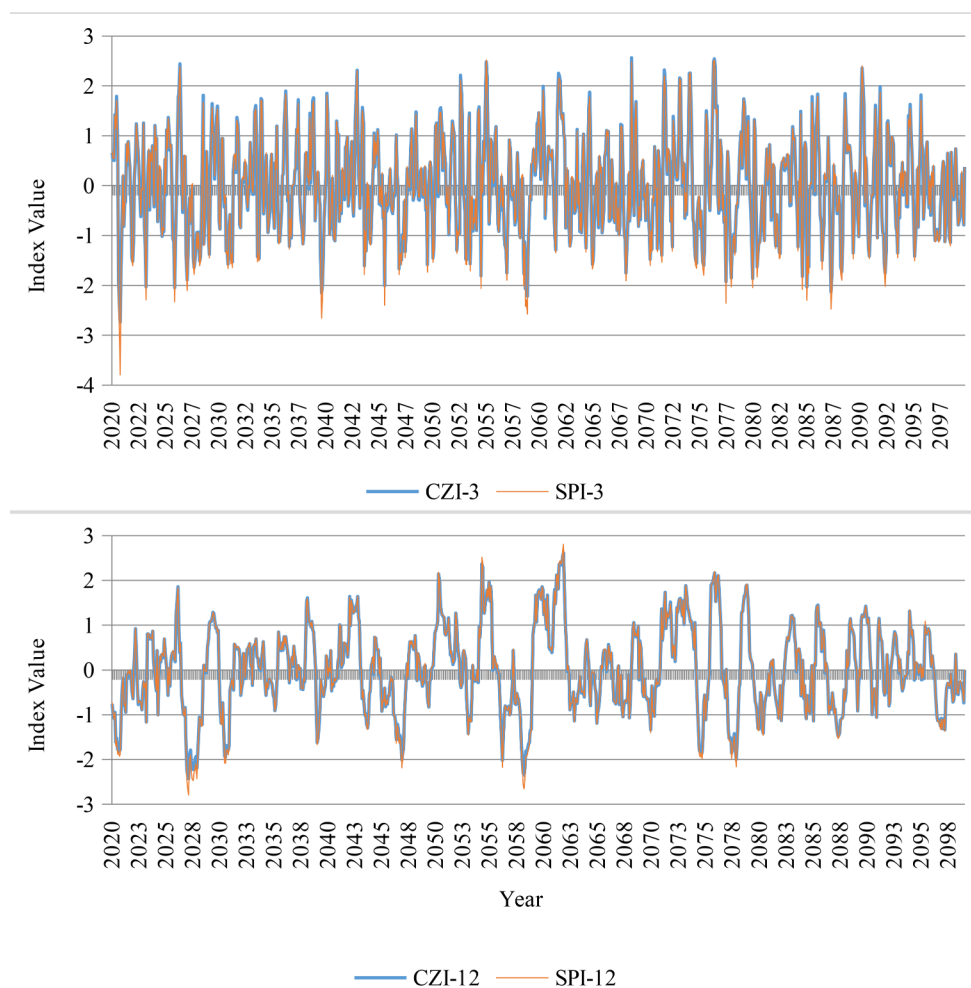

a spatial increase in drought events spreading from west to east, and the eastern region will experience drought lasting for 45–50 months. Across the study area, a 50–55 month drought is predicted in the late century; in small areas in the north and east, this value decreases to 40–45 months, while in a small area in the west, it increases to 55–60 months.

Figure 9 shows the spatial distribution of the number of months experiencing severe drought. According to the SPI-3 index, the total duration of severe drought, which is expected last for 15–18 months in the western half of the study area in the near future, increases to 21–24 months in the eastern half under the SSP2-4.5 climate change scenario. In the mid-century, it is predicted that there will be a drought of 12–15 months in general at the eastern and western ends, and a general drought of 9–12 months in the middle part. A severe drought is predicted to last for 12–15 months in the northern region of the study area and 15–18 months in general in the remaining regions in the late century. According to the SPI-12 index, on the other hand, it is predicted that there will be a drought lasting 21–24 months in the central part of the area in the near future. This value tends to decline in the eastern and western parts of the area, decreasing to 15

to 18 months. In the mid-century, the area will experience a drought of 6–9 months, 9–12 months in the eastern end, 12–15 months in some regions, and 3–6 months in some regions in the west. In the late century, it is predicted that the eastern half of the region would experience a drought lasting 9–12 months and the western half will experience a drought lasting 12–15 months.

According to the SPI-3 index, the SSP5-8.5 scenario predicts that the entire region will experience a 3–6 months drought in the near future. It is anticipated that there will be 15–18 months of drought at the eastern and western ends of the region throughout the mid-century and 18–21 months of drought in the remaining central part. In the western half of the region, drought is predicted to last for 21–24 months in the late century, whereas in the eastern half, drought is predicted to last between 18 and 27 months in certain regions. According to the SPI-12 indicator, 0 to 3 months of drought are predicted for the entire region in the near future. It is interesting that in the mid-century, the regions in the middle of the region that experience drought for 21–24 months will comprise a large area, and the number of dry months in the eastern and western parts will decrease by 12–15 months. It

Fig. 7 SPI and CZI index time series according to SSP5-8.5 scenario
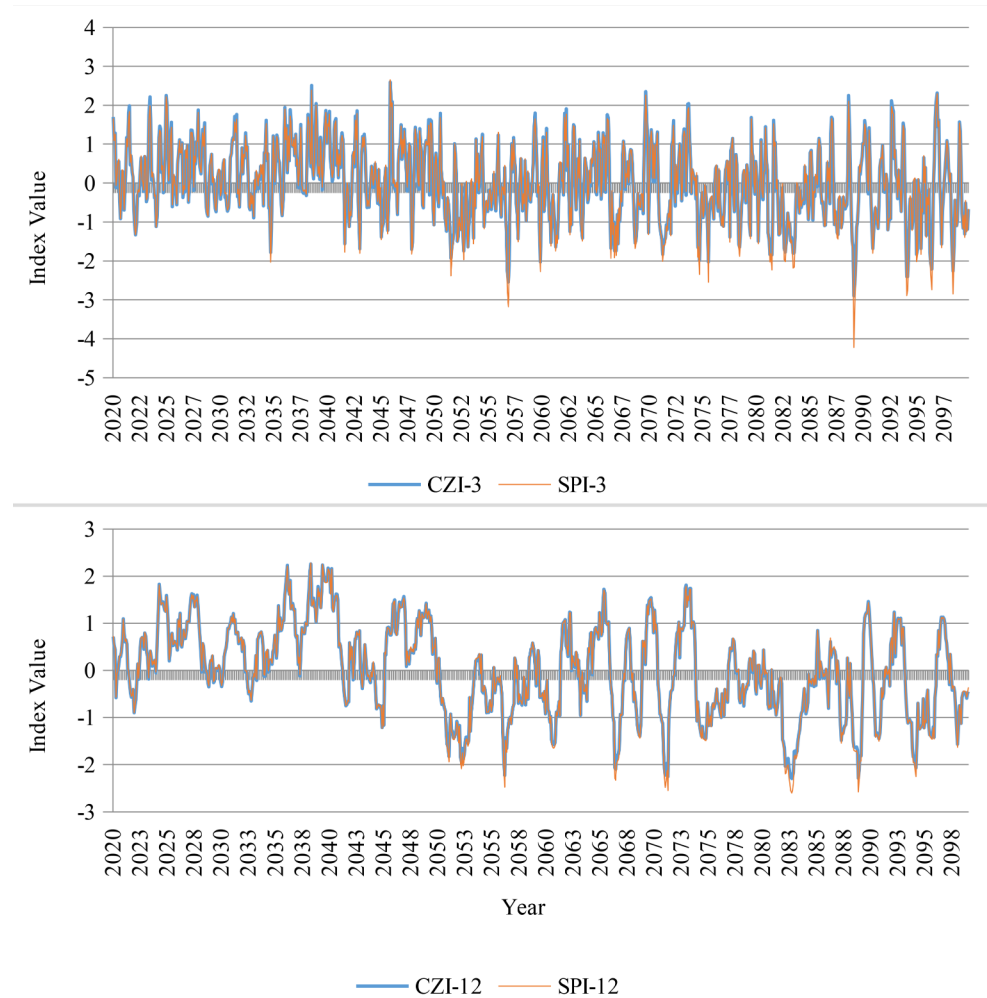

is noteworthy in the mid-century, the regions in the middle of the region that experience drought for 21–24 months will comprise a large area, and the number of dry months in the eastern and western parts will decrease by 12–15 months.

Figure 10 depicts the spatial distribution of the number of months that will experience extreme drought Under the SSP2-4.5 scenario, the SPI-3 index predicts an extreme drought lasting 10–12 months in a strip-shaped area in the center of the region and 8–10 months in the remaining region. In the mid-century, a small area in the west will experience a drought lasting 2–4 months, while the entire region will be affected by a drought lasting 4–6 months. On the other hand, towards the late century, 8–10 months of drought are predicted in the eastern part of the region and 6–8 months in the remaining region. According to the SPI-12 index, a more severe drought is predicted. In the near future, approximately one-third of the region is expected to experience droughts lasting 16–18 months, one-third will experience droughts lasting 14–16 months, and the remaining portion will experience droughts lasting 10–14 months. While the eastern half of the region is predicted to

experience a drought lasting 4–6 months in the mid-century, there are regions that are predicted to experience drought on a varying scale, such as 2–10 months in the western half. While most of the region is predicted to experience a drought of 0–4 months in the late century, it is noteworthy that this value increases to 12–14 months at the western end.

Under the SSP5-8.5 scenario, according to the SPI-3 index, extreme drought is expected to last 2–4 months in the northern and eastern ends of the area and 4–6 months in the rest of the area in the near future. In the mid-century, it is predicted that there will be a drought lasting 10–12 months in the north end, 6–8 months in the east end, and 8–10 months in the remaining part. In the late century, it is anticipated that the western region will experience 18–20 months of drought, and the remaining regions will experience 14–18 months. In the near future, the SPI-12 index predicts that the entire region will experience a drought lasting 0–2 months. It is expected that in the mid-century, wide-ranging droughts lasting 6 to 18 months will occur in various parts of the area. While a 14–16 months drought is predicted for
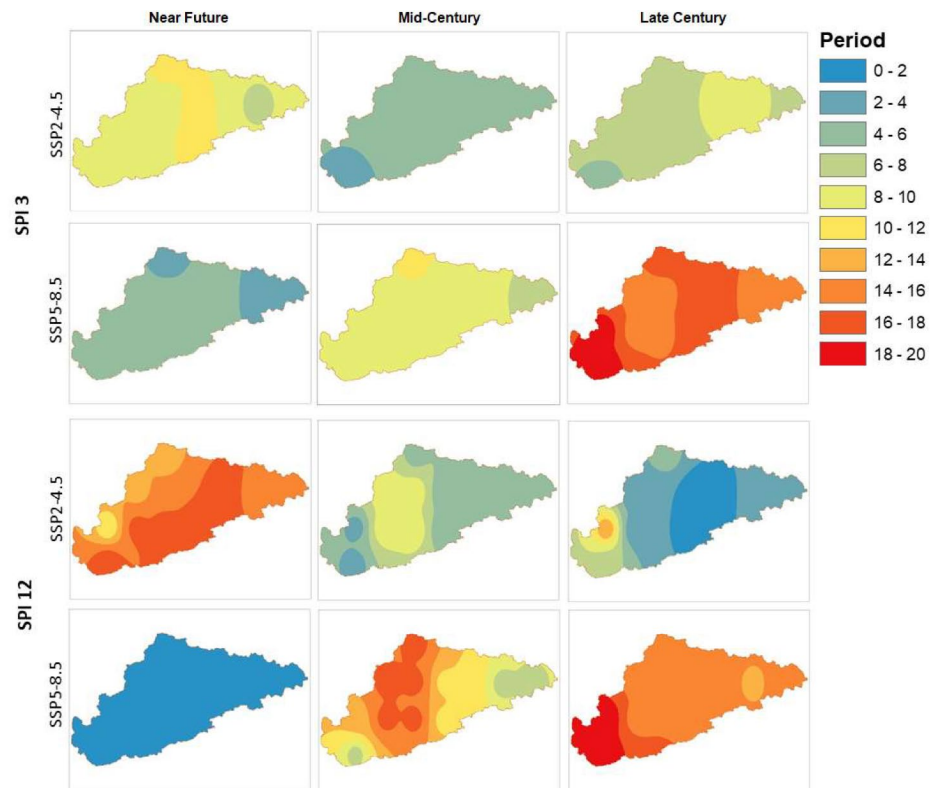
Fig. 8 Spatial distribution maps of the number of months that will experience moderate droughts (−1.0 ≥ SPI > −1.5)
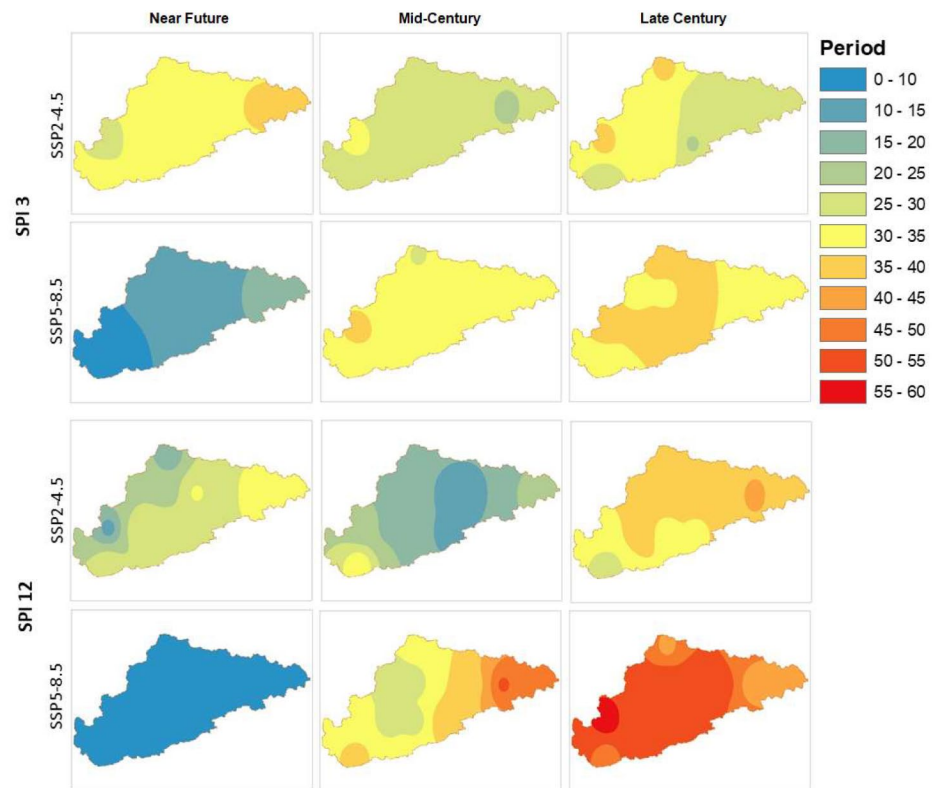
Fig. 9 Spatial distribution maps of the number of months that will experience severe drought (−1.5 ≥ SPI > −2.0)
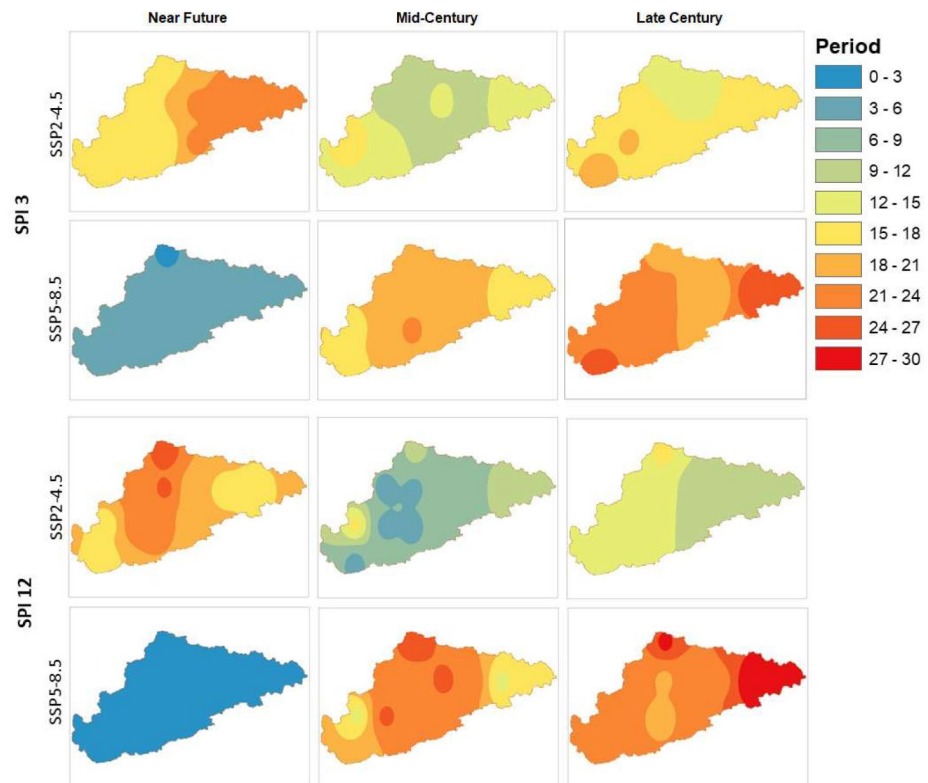
Fig. 10 Spatial distribution maps of the number of months that will experience extreme drought (-2.0 ≥ SPI)

most of the area in the late century, it is notable that the western end will experience an 18–20 month drought.

4 Conclusion

Within the scope of this study, a prediction was made for drought events in the Upper Kızılırmak basin that may occur under the SSP 2-4.5 and SSP 5-8.5 climate change scenarios. Precipitation data from the CC-CSM2-MR, GFDL-ESM4, INM-CM5-0, and MRI-ESM2 global climate models were subjected to statistical downscaling and error correction using the CCT software. SPI-3 and SPI-12 indexes were calculated for the years 2020–2100 using the recently acquired data set. Time series graphs were generated for SPI indexes for the near future (2020–2049), the mid-century (2050–2074), and the late century (2075–2099), and drought events were subjected to trend analysis. Spatial distribution maps were created by the interpolation method utilizing the total number of dry months in order to examine the spatial distribution of the predicted drought events. These maps were created and evaluated separately for the classifications of moderate drought (-1.0 SPI > -1.5), severe drought (-1.5 SPI > -2.0), and extreme drought (-2.0 SPI).

According to the trend analysis results, there will be no statistically significant trend in drought events in the SSP

2-4.5 climate change scenario. In the SSP 5-8.5 scenario, there will be a statistically significant decreasing trend in drought events in the medium future according to SPI-3 and SPI-12 indices.

Based on the interpretation of the SPI time series graphics, it has been determined that the SSP 2-4.5 climate change scenario will experience the most severe drought events in the near future, while precipitation anomalies will decrease as the end of the review period approaches. According to the SPI-3 index, in particular, SPI values will become near 0 and remain in the range of -1 < SPI < 1, and precipitation anomalies will become essentially nonexistent in the final months of the investigation period. There will be no significant drought anomalies until the half of the recent period. However, starting from the middle of this period, the number and severity of precipitation anomalies and the duration of dry periods will increase.

Comparison of SPI and CZI data showed that both indices are effective in assessing drought conditions and meteorological drought analyses. This comparative analysis makes a significant contribution to improving the accuracy and reliability of methodologies used in drought research.

Spatial distribution analysis revealed that moderate drought events will exhibit a spatial distribution ranging from 0 to 60 months throughout different examination periods. In both climate change scenarios, moderate drought events will last longer than the SPI-3 index compared to

the SPI-12 index. Moderate drought events will be more effective in the SSP 5-8.5 scenario in the late the century. According to the SPI-3 index, which offers an indication of the influence of drought on soil moisture, while the central parts of the basin will be more affected by this condition, the eastern and western ends will be less affected. According to the SPI-12 index, which is an indicator of the impact of drought on water reserves, the drought's impact area will be larger than SPI-3, affecting roughly 80% of the area. Severe drought events will exhibit a spatial distribution on a scale varying from 0 to 30 months. Under the SSP 5-8.5 scenario, the most effective droughts will occur in the late century. According to the SPI-3 and SPI-12 indexes, the spatial distribution scale of drought events is similar throughout this time period. The region most affected by the drought events will be at the western end which will make up 20% of the study area. Given that this region is where the Kızılırmak river originates, the potential meteorological drought will impact the entire river flow. Moreover, extreme drought events will exhibit a spatial distribution ranging between 0 and 20 months. Under the SSP 5-8.5 scenario, the most effective drought events will occur in the late century. According to the SPI-3 index, drought events will last longer than SPI-12 during this period. Both indexes indicate that the western end of the study area will experience the longest duration of drought.

This study emphasizes the predicted changes in meteorological drought anomalies in relation to the effects of climate change. In light of these projections, future studies should focus on the dangers that drought events pose to agriculture, food security, and the sustainable use of water resources, as well as the preventative measures that can be taken. However, the study acknowledges that the climate models, scenario assumptions and methodological approaches used when presenting projections of meteorological drought events under climate change scenarios have their own uncertainties.

Declarations

References

Afshar MH, Şorman AÜ, Tosunoğlu F, Bulut B, Yilmaz MT, Danandeh Mehr A (2020) Climate change impact assessment on mild and extreme drought events using copulas over Ankara, Turkey. Theoretical Appl Climatology 141(3):1045–1055. https://doi.org/10.1007/s00704-020-03257-6

Anuchaivong P, Sukawat D, Luadsong A (2017) Statistical downscaling for Rainfall forecasts using modified constructed Analog Method in Thailand. Sci World J 2017:1075868. https://doi.org/10.1155/2017/1075868

Asong ZE, Khaliq MN, Wheater HS (2016) Multisite multivariate modeling of daily precipitation and temperature in the Canadian Prairie provinces using generalized linear models. Clim Dyn 47(9):2901–2921. https://doi.org/10.1007/s00382-016-3004-z

Azizi H, Nejatian N (2022) Evaluation of the climate change impact on the intensity and return period for drought indices of SPI and SPEI (study area: Varamin plain). Water Supply 22(4):4373–4386. https://doi.org/10.2166/ws.2022.056

Blanco-Gómez P, Jimeno-Sáez P, Senent-Aparicio J, Pérez-Sánchez J (2019) Impact of Climate Change on Water Balance Components and droughts in the Guajoyo River Basin (El Salvador). Water 11:2360. https://doi.org/10.3390/w11112360

Bolch T, Kulkarni A, Kääb A, Huggel C, Paul F, Cogley J, Scheel M (2012) The state and fate of himalayan glaciers. Sci 336(6079):310–314. https://doi.org/10.1126/science.1215828

Bong CHJ, Richard J (2020) Drought and climate change assessment using standardized precipitation index (SPI) for Sarawak River Basin. J Water Clim Change 11(4):956–965. https://doi.org/10.2166/wcc.2019.036

Circi Selcuk B, Irmak MA (2022) A study on the adequacy and requirement of urban active green areas in Sivas. Fresenius Environ Bull 31(02):2209–2220

Corell R (2007) Downscaling: An Imperative to Assess Climate Change at Regional to Local Scales. Workshop on Adaptation of Climate Scenarios to Arctic Climate Impact Assessments, May 14–16, Oslo.

Crane RG, Hewitson BC (1998) Doubled CO_2 precipitation changes for the Susquehanna Basin: down-scaling from the genesis general circulation model. International J Climatology 18(1):65–76. https://doi.org/10.1002/(SICI)1097-0088(199801)18:13.0.CO;2-9

Danandeh Mehr A, Sorman AU, Kahya E, Hesami Afshar M (2020) Climate change impacts on meteorological drought using SPI and

SPEI: case study of Ankara, Turkey. Hydrol Sci J 65(2):254–268. https://doi.org/10.1080/02626667.2019.1691218

Dile YT, Srinivasan R (2014) Evaluation of CFSR climate data for hydrologic prediction in data-scarce watersheds: an application in the Blue Nile River Basin. J Am Water Resour Association (JAWRA) 50(5):1–16. https://doi.org/10.1111/jawr.12182

Dosio A, Paruolo P (2011) Bias correction of the ENSEMBLES high-resolution climate change projections for use by impact models: evaluation on the present climate. J Geophys Res Atmos 116(22):1–22. https://doi.org/10.1029/2011JD015934

Edwards DC, McKee TB (1997) Characteristics of 20th century drought in the United States at multiple time scales. Climatology Report 97–2, Department of Atmospheric Science, Colorado State University, Fort Collins CO

Ercan B, Yüce Mİ (2017) Trend Analysis of Hydro-Meteorological variables of Kızılırmak Basin. Nevsehir J Sci Technol 6:333–340. ICOCEE 2017 Special Issuehttps://doi.org/10.17100/nevbiltek.323640

Gomez-Gomez JF, Pulido-Velazquez D, Collados-Lara AJ, Fernandez-Chacon F (2022) The impact of climate change scenarios on droughts and their propagation in an arid Mediterranean basin. A useful approach for planning adaptation strategies. Sci Total Environ 820:153128. https://doi.org/10.1016/j.scitotenv.2022.153128

Gudmundsson L, Seneviratne SI (2016) Anthropogenic climate change affects meteorological drought risk in Europe. Environ Res Lett 11(4):044005. https://doi.org/10.1088/1748-9326/11/4/044005

Hagemann S, Chen C, Haerter JO, Heinke J, Gerten D, Piani C (2011) Impact of a statistical bias correction on the projected hydrological changes obtained from three GCMs and two hydrology models. J Hydrometeorology 12(4):556–578. https://doi.org/10.1175/2011JHM1336.1

Hamed KH, Rao AR (1998) A modified Mann-Kendall trend test for autocorrelated data. J Hydrology 204(1–4):182–196. https://doi.org/10.1016/S0022-1694(97)00125-X

Hayes M, Svoboda M, Wall N, Widhalm M (2011) The Lincoln Declaration on drought indices: universal meteological drought index recommended. Bull Am Meteorical Soc 92(4):485–488

IPCC (2013) In: Stocker TF, Qin D, Plattner GK, Tignor M, Allen SK, Boschung J et al (eds) Climate Change 2013: the physical science basis. Contribution of Working Group I to the Fifth Assessment Report of the Intergovernmental Panel on Climate Change. Cambridge University Press, Cambridge, United Kingdom and New York, NY, USA

IPCC (2021) In: Masson-Delmotte V, Zhai P, Pirani A, Connors SL, Péan C, Berger S, Caud N et al (eds) Climate Change 2021: the physical science basis. Contribution of Working Group I to the Sixth Assessment Report of the Intergovernmental Panel on Climate Change. Cambridge University Press, Cambridge, United Kingdom and New York, NY, USA. https://doi.org/10.1017/9781009157896

John JG, Blanton C, McHugh C et al (2018) NOAA-GFDL GFDL-ESM4 model output prepared for CMIP6. https://doi.org/10.22033/ESGF/CMIP6.8691. Earth System Grid Federation

Kelley CP, Mohtadi S, Cane MA, Seager R, Kushnir Y (2015) Climate change in the Fertile Crescent and implications of the recent Syrian drought. Proc Natl Acad Sci 112(11):3241–3246. https://doi.org/10.1073/pnas.1421533112

Kendall MG (1975) Rank correlation methods. Griffin, London, UK

Kendall MG, Stuart A (1977) The Advanced Theory of statistics. Charles Griffin & Company, London, High Wycombe

Knutson TR, Zeng F (2018) Model assessment of observed precipitation trends over land regions: detectable human influences and possible low bias in model trends. J Clim 31(12):4617–4637. https://doi.org/10.1175/JCLI-D-17-0672.1

Lee SH, Yoo SH, Choi JY, Bae S (2017) Assessment of the impact of climate change on drought characteristics in the Hwanghae Plain,

North Korea using time series SPI and SPEI: 1981–2100. Water 9(8):579

Lornezhad E, Ebrahimi H, Rabieifar HR (2023) Analysis of precipitation and drought trends by a modified Mann–Kendall method: a case study of Lorestan province, Iran. Water Supply 23(4):1557–1570. https://doi.org/10.2166/ws.2023.068

Mann HB (1945) Nonparametric tests against trend. Econometrica 13:245–259. https://doi.org/10.2307/1907187

McKee TB, Doesken NJ, Kleist J (1993) The relationship of drought frequency and duration to time scale. In: Proceedings of the Eighth Conference on Applied Climatology, Anaheim, California, 17–22 January 1993, 179–184

Merabti A, Martins DS, Meddi M, Pereira LS (2018) Spatial and time variability of drought based on SPI and RDI with various time scales. Water Resour Manage 32:1087–1100. https://doi.org/10.1007/s11269-017-1856-6

Ndhlovu GZ, Woyessa YE (2021) Use of gridded climate data for hydrological modelling in the Zambezi River Basin, Southern Africa. J Hydrology 602:126749. https://doi.org/10.1016/j.jhydrol.2021.126749

Sağdıç M, Koç H (2012) Climate of the Upper Kızılırmak Basin. Turkish Geographical Rev 58:1–20 (In Turkish)

Saha S, Moorthi S, Pan HL, Wu X, Wang J, Nadiga S et al (2010) The NCEP climate forecast system reanalysis. Bull Am Meteorol Soc 91(8):1015–1057. https://doi.org/10.1175/2010BAMS3001.1

Selçuk SF, Cebeci MS, Cerit O, Selçuk BÇ, Karagözoğlu MB (2022) Climate change projections of Sivas province. Nigde Omer Halisdemir Univ J Eng Sci 11(3):522–533 (In Turkish). https://doi.org/10.28948/ngumuh.1091466

Sen B, Topcu S, Türkeş M, Sen B, Warner JF (2012) Projecting climate change, drought conditions and crop productivity in Turkey. Clim Res 52:175–191. https://doi.org/10.3354/cr01074

Sen PK (1968) Estimates of the regression coefficient based on Kendall's tau. J Am Stat Association 63(324):1379–1389

Singh VK, Kumar D (2020) Downscaling daily precipitation over the Upper Shivnath basin: a comparison of three statistical downscaling techniques. Int J Curr Microbiol Appl Sci 9(1):1676–1688. https://doi.org/10.20546/ijcmas.2020.901.185

Timbal B, Fernandez E, Li Z (2009) Generalization of a statistical downscaling model to provide local climate change projections for Australia. Environ Modelling Softw 24:341–358. https://doi.org/10.1016/j.envsoft.2008.07.007

Tramblay Y, Koutroulis A, Samaniego L, Vicente-Serrano SM, Volaire F, Boone A et al (2020) Challenges for drought assessment in the Mediterranean region under future climate scenarios. Earth-Sci Rev 210:103348. https://doi.org/10.1016/j.earscirev.2020.103348

Türkeş M (2012) Observed and projected Climate Change, Drought and Desertification in Turkey. Ankara Univ J Environ Sci 4(2):1–32 (In Turkish)

Türkeş M (2019) Climate Change Education Modules Series 1: Scientific Basis of Climate Change, Effects on Turkey, 1st Edition. WEglobal Danışmanlık AŞ, Ankara,Turkey. (In Turkish)

Vaghefi S, Abbaspour N, Kamali B, Abbaspour KC (2017) A toolkit for climate change analysis and pattern recognition for extreme weather conditions – case study: California-Baja California Peninsula. Environ Modelling Softw 96:181–198. https://doi.org/10.1016/j.envsoft.2017.06.033

Volodin E, Mortikov E, Gritsun A et al (2019) INM INM-CM5-0 model output prepared for CMIP6. https://doi.org/10.22033/ESGF/CMIP6.12330. Earth System Grid Federation

Wu H, Hayes MJ, Weiss A, Hu QI (2001) An evaluation of the standardized precipitation index, the China-Z Index and the statistical Z-Score. Int J Climatology: J Royal Meteorological Soc 21(6):745–758. https://doi.org/10.1002/joc.658

Xin X, Wu T, Shi X et al (2019) BCC BCC-CSM2MR model output prepared for CMIP6. https://doi.org/10.22033/ESGF/CMIP6.3035. Earth System Grid Federation

Yukimoto S, Koshiro T, Kawai H et al (2019) MRI MRI-ESM2.0 model output prepared for CMIP6. https://doi.org/10.22033/ESGF/CMIP6.6915. Earth System Grid Federation

Zhang Q, Li J, Singh VP, Bai Y (2012) SPI-based evaluation of drought events in Xinjiang, China. Nat Hazards 64:481–492. https://doi.org/10.1007/s11069-012-0251-0